

Supporting information

“Flow-dependent separation selectivity for organic molecules on metal-organic framework containing adsorbents”

Anton Peristy, Pavel N. Nesterenko, Anita Das, Deanna M. D'Alessandro, Emily F. Hilder and R. Dario Arrua*

Materials

5 μm microspherical silica particles Nucleosil 300-5 were obtained from Macherey-Nagel GmbH & Co. KG, Germany. Toluene, 3-(glycidyloxypropyl)trimethoxysilane, glutamic acid (Glu), 1,4-benzenedicarboxylic acid (H_2bdc , 98%) were purchased from Sigma-Aldrich (St Louis, MO, USA). Zirconium chloride (anhydrous) was obtained from Merck (Schuchardt, Germany). Dimethylformamide (DMF) and hydrochloric acid (32%) were purchased from Univar Ajax Finechem, NSW, Australia. HPLC grade *n*-hexane, 2-propanol, and dimethylformamide (all from Sigma-Aldrich, St Louis, MO, USA) were used for packing of stainless steel column and HPLC experiments. Solutions of pure reagents (>99%, Sigma-Aldrich, St Louis, MO, USA) were used as model solutes in chromatographic experiments.

Instrumentation

PXRD measurements were performed on a PAN Analytical X'pert Pro diffractometer fitted with a solid-state PIXcel detector (40 kV, 30 mA, 1° divergence and anti-scatter slits, and 0.3 mm receiver and detector slits) using $\text{Cu-K}\alpha$ ($\lambda = 1.5406 \text{ \AA}$) radiation. Scanning electron microscopy (SEM) images of the particles were performed using a FEI Quanta 600 MLA ESEM in the Central Science Laboratory, University of Tasmania (Australia). The particles were sputter-coated with platinum. Chromatographic separations were performed using Water 2490 HPLC system equipped with Water 2487 UV detector (Milford, MA, USA)

Synthesis of SiO₂-Glu

The 5 μm silica particles with bonded glutamic acid functional groups were prepared as previously described.¹ At first step, 2.45 g of silica particles were suspended in 30 mL solution of 3-(glycidyloxypropyl)-trimethoxysilane (3.4 wt/vol %) in toluene. This suspension was refluxed for 24 h using an overhead stirrer. After the reaction the obtained silica particles modified with epoxy- groups were washed with 100 mL of acetone, 400 mL of ethanol and dried under vacuum. On a second step, 2 g of the epoxy-modified silica particles were suspended in 50 mL aqueous solution of glutamic acid (1.35 wt/vol %). Before the addition of the particles, the pH of the solution was adjusted to 9.4 using a concentrated solution of NaOH. The ring opening reaction was allowed to proceed under reflux for 2.5 h using an overhead stirrer. The prepared silica particles with bonded glutamic acid were washed using the same procedure described above and dried under vacuum.

Synthesis of UiO-66 crystals

The synthesis of UiO-66 nanocrystals was carried out by a microwave-assisted solvothermal synthesis² using an Anton-Paar Monowave 300 microwave oven. A 30 mL glass microwave vial was charged with 0.50 mmol ZrCl₄ (> 99.9%, Sigma-Aldrich), 4 mL of concentrated HCl and 10 mL of *N,N'*-dimethylformamide (DMF). The solution was stirred for 30 min before 0.5 mmol of 1,4-benzenedicarboxylic acid (H₂bdc, 98%, Sigma-Aldrich) was added to the mixture. The suspension was placed within the microwave oven and heated with magnetic stirring to 160 °C within 30 min, and held at this temperature for 40 min before cooling to 55 °C within 1 min. The UiO-66 crystals were washed by centrifugation with portions of 20 mL DMF (6000 rpm, 3 times for 5 minutes) and 20 mL acetone (6000 rpm, 3 times for 5 minutes). Finally, the UiO-66 crystals were dried under vacuum.

Synthesis of UiO-66@SiO₂ core-shell particles

The deposition of UiO-66 nanocrystals on carboxylic acid-modified silica particles was performed using the same method described above for the synthesis of UiO-66 crystals but in the presence of SiO₂-Glu particles. A 30 mL glass microwave vial was charged with 0.35 mg of modified silica particles, 0.50 mmol ZrCl₄, 4 mL of concentrated HCl and 10 mL *N,N'*-dimethylformamide (DMF). The suspension was stirred for 30 min before 0.5 mmol of H₂bdc was added to the mixture. The suspension was placed within the microwave oven and heated

with magnetic stirring to 160 °C within 30 min, and held at this temperature for 40 min before cooling to 55 °C within 1 min. The modified particles and UiO-66 nanocrystals were washed by centrifugation with portions of 20 mL DMF (6000 rpm, 3 times for 5 minutes) and 20 mL acetone (1000 rpm, 6 times for 1 minute). The washes with acetone at lower speeds allowed the separation of UiO-66 nanocrystals and the modified core-shell particles due to their difference in density. The resulting particles were dried under vacuum. A second deposition step of UiO-66 was performed onto the core-shell particles by following the same procedure as described above.

Packing procedure

UiO-66@SiO₂ particles were packed within 50 × 2.1 mm ID stainless steel column. The system for column packing consisted of a Haskel DSF-122 air driven liquid pump (Haskel International Inc., Burbank, CA, USA), and connected in series 150 × 4.6 mm ID stainless steel slurry reservoir (volume 2.5 mL, purchased from Phenomenex, Lane Cove West, NSW, Australia), a 50 × 2.1 mm ID column extension and a 50 × 2.1 mm ID empty column with 0.5 μm pore size frits (all from Restek, Bellefonte, PA, USA). Slurry containing 0.10 g·mL⁻¹ of UiO-66@SiO₂ was prepared in DMF. Slurry concentration was chosen considering the packing density of unmodified 5 μm Nucleosil (pore diameter 30 nm)^{3,4,4} of less than 1.1 g·mL⁻¹ with 25% excess, and the volume of reservoir of 2.5 mL. Empty column and column extension were filled with pure DMF in order to avoid bubbles, which may cause erratic slurry movements under the packing pressure. Slurry was placed in the reservoir, and 2-propanol was used as a pump fluid.

During the packing, the pump was operated manually and the pressure program included a fast increase from 0 to 6000 psi within 3-5 seconds at the beginning of packing. Subsequently, pressure was held at a target level of 6000 psi until ~100 mL of 2-propanol was pumped through the column. Then the pump was turned off and after the pressure had dropped down to 0 psi (within 2-3 mins), the column was disconnected from the extension and the top frit and fitting were installed.

Determination of the void times, retention times, retention factors and selectivities.

Void time (t_0) was measured via disturbance on the base line, related to the injection. In the cases when baseline disturbance was not evident, additional blank injections were done (in triplicates) at each flow rate in order to record the void time.

Retention times (t_R) were recorded at the peak maximum, and retention factors (k) were calculated as $k = (t_R - t_0)/t_0$. Selectivity (α) was calculated as $\alpha = k_1/k_2$.

As mentioned in the main manuscript, an intriguing variation of the column void volume (V_0 , calculated as $V_0 = t_0 \cdot F$, where F is the mobile phase flow rate) with the flow rate was observed. For example, with the increase of the mobile phase flow rate from 0.03 to 1.5 mL·min⁻¹ the V_0 value increased by 60%. This effect is surprising, considering the fact that in chromatography the void volume is defined as the volume of the mobile phase in the column, and it cannot depend on the flow rate.⁵ As said, the V_0 value is obtained by simple multiplying the time of the disturbance of the baseline by the flow rate, and its variation implies that in these conditions the disturbance of the baseline travels through the column with a rate different from the mobile phase flow rate. Accordingly, what was measured is not the void volume in the common sense, but rather an apparent void volume V_0^{app} .

The 60% increase for the measured V_0^{app} value is rather large, but it is consistent for the injections of different analytes at different flow rates, using several UiO-66@SiO₂ columns. There can be at least two reasons which may affect the apparent column void volume at different flow rates. First, the kinetic diameter of the hexane molecule of the mobile phase is 0.602 nm (see Table 1S), which is comparable to that of toluene and ethyl benzene. Therefore, the possibility should be considered that the diffusion of the hexane into micropores on UiO-66 is also affected by the FDSS effect, similarly to toluene and ethyl benzene. In this case, at different flow rates different proportion of internal porosity of UiO-66 is accessible by the mobile phase, and, obviously the apparent void volume may vary. Furthermore, based on the SEM images of particles (Fig. 1S), it is clear the UiO-66 layer is primarily on the surface of the silica beads, meaning that significant part of mesopores in silica may be blocked by MOF layer. It was previously shown by Sorribas *et al.*⁶ that in similar core-shell ZIF-8@SiO₂ particles the diffusion inside SiO₂ particles was limited by the diffusion through the micropores of the ZIF-8 shell. If similar assumption is valid for UiO-66@SiO₂ particles, it means that FDSS effect is likely to take place in pores of both silica and MOF, thus increasing the V_0^{app} variation with the flow rate. Additionally, increase in the flow rate is achieved by rise in pressure, which in turn provides easier access of mobile size to the silica pores under MOF layer, which may be otherwise inaccessible at lower flow

rates. This assumption is also partially confirmed by the fact the equilibrating of UiO-66@SiO₂ column was always taking extremely long flushing with mobile phase (over 500 column volumes) in order to achieve stable retention times at each flow rate.

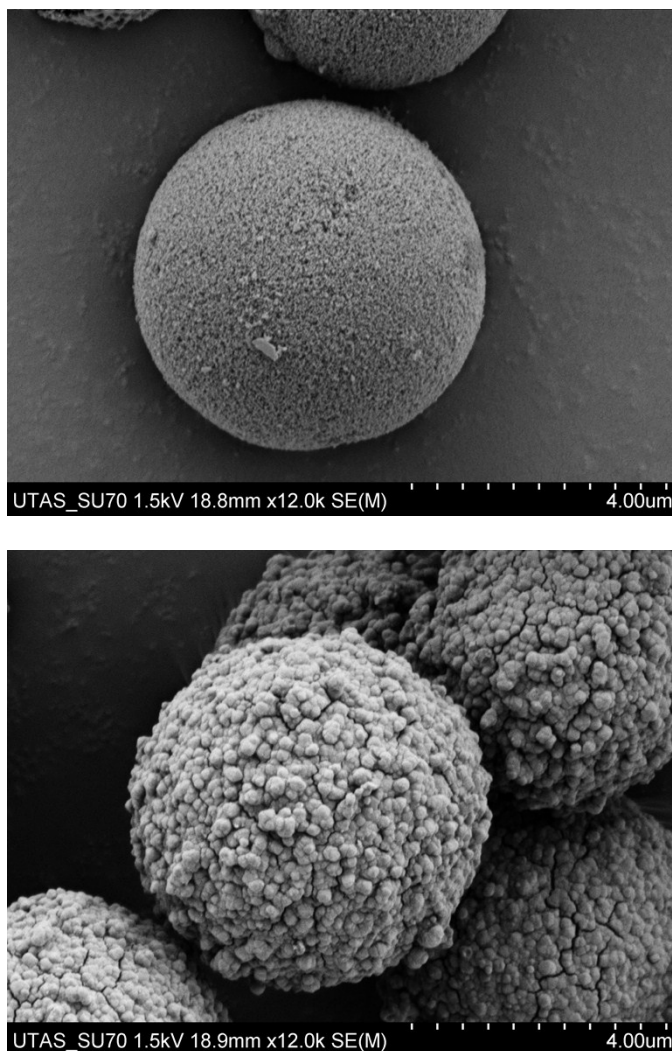


Fig. 1S. Scanning electron microscopy images of SiO₂-Glu (top) and UiO-66@SiO₂ (bottom) particles.

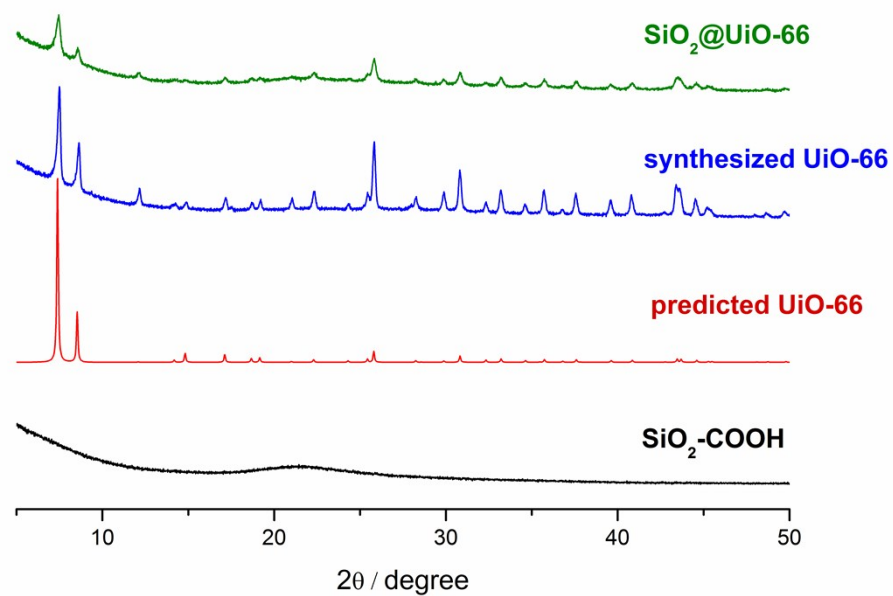


Figure 2S. PXRD patterns of SiO₂-Glu (black), predicted UiO-66 (red), synthesized UiO-66 (blue) and UiO-66@SiO₂ core-shell particles (green)

Table 1S. Retention factors for different solutes on UiO-66@SiO₂ column and their calculated kinetic diameters (σ , nm). Retention data obtained in *n*-hexane mobile phase at 25°C and flow rate of 0.2 mL·min⁻¹, and σ values calculated as suggested by Jae et al.⁴, using critical data from ^{7,8}.

	Substance	M _w , g·mol ⁻¹	<i>k</i>	σ , nm	Ref.
	<i>n</i> -Hexane	86	-	0.602	5
7	Pentyl benzene	148	0.21	0.687	6
6	Butyl benzene	134	0.33	0.666	5
5	Propyl benzene	120	0.41	0.640	5
13	Biphenyl	154	0.44	0.666	5
4	Cumene	120	0.63	0.636	6
1	Benzene	78	1.00	0.534	5
3	Ethyl benzene	106	1.27	0.606	5
10	<i>p</i> -Xylene	106	1.33	0.608	6
15	Anthracene	178	1.46	0.691	5
8	Styrene	104	1.47	0.603	6
2	Toluene	92	1.86	0.573	5
11	<i>m</i> -Xylene	106	2.04	0.606	5
9	Phenyl acetylene	102	3.27	0.581	6
12	<i>o</i> -Xylene	106	5.17	0.604	5
14	Naphthalene	128	6.10	0.623	5

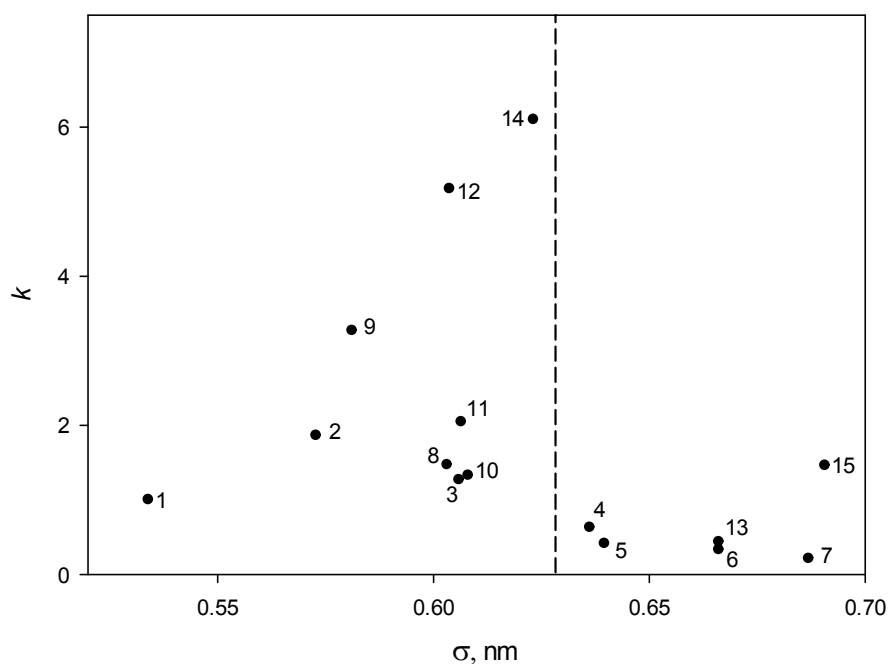


Figure 3S. Relationship between analyte molecules kinetic diameter and their retention on UiO-66@SiO₂ column. Experimental conditions and data points as in the Table S1.

- 1 A. I. Elefterov, M. G. Kolpachnikova, P. N. Nesterenko and O. A. Shpigun, *J. Chromatogr. A*, 1997, **769**, 179.
- 2 X. Q. Zhang, Q. Han and M. Y. Ding, *RSC Adv.*, 2015, **5**, 1043.
- 3 P. N. Nesterenko, Personal communication, 2015,
- 4 J. Jae, G. A. Tompsett, A. J. Foster, K. D. Hammond, S. M. Auerbach, R. F. Lobo and G. W. Huber, *J. Catal.*, 2011, **279**, 257.
- 5 G. Guiochon, D. G. Shirazi, A. Felinger, A. M. Katti, *Fundamentals of Preparative and Nonlinear Chromatography*, Academic Press, Cambridge, MA, 2006.
- 6 S. Sorribas, B. Zornoza, C. Tellez and J. Coronas, *Chem. Commun.*, 2012, **48**, 9388.
- 7 D. R. Lide, *CRC Handbook of Chemistry and Physics*, CRC Press/Taylor and Francis, Boca Raton, FL, 2010.
- 8 www.infotherm.com/, *Infotherm Thermophysical Database*, Wiley Information Services GmbH, 2014.